Journal of the American College of Cardiology
© 2010 by the American College of Cardiology Foundation
Published by Elsevier Inc.

Vol. 56, No. 9, 2010
ISSN 0735-1097/$36.00
doi:10.1016/j.jacc.2010.03.066

PRE-CLINICAL RESEARCH

Guided Cardiopoiesis Enhances Therapeutic Benefit of Bone Marrow Human Mesenchymal Stem Cells in Chronic Myocardial Infarction

Atta Behfar, MD, PHD,* Satsuki Yamada, MD, PHD,* Ruben Crespo-Diaz, BS,* Jonathan J. Nesbitt, BS,* Lois A. Rowe, ASCP,* Carmen Perez-Terzic, MD, PHD,*† Vinciane Gaussin, PHD,‡ Christian Homsy, MD,‡ Jozef Bartunek, MD, PHD,§ Andre Terzic, MD, PHD*

Rochester, Minnesota; and Mont-Saint-Guibert and Aalst, Belgium

Objectives The goal of this study was to guide bone marrow-derived human mesenchymal stem cells (hMSCs) into a cardiac progenitor phenotype and assess therapeutic benefit in chronic myocardial infarction.

Background Adult stem cells, delivered in their naïve state, demonstrate a limited benefit in patients with ischemic heart disease. Pre-emptive lineage pre-specification may optimize therapeutic outcome.

Methods hMSC were harvested from a coronary artery disease patient cohort. A recombinant cocktail consisting of transforming growth factor-beta$_1$, bone morphogenetic protein-4, activin A, retinoic acid, insulin-like growth factor-1, fibroblast growth factor-2, alpha-thrombin, and interleukin-6 was formulated to engage hMSC into cardiopoiesis. Derived hMSC were injected into the myocardium of a nude infarcted murine model and followed over 1 year for functional and structural end points.

Results Although the majority of patient-derived hMSC in their native state demonstrated limited effect on ejection fraction, stem cells from rare individuals harbored a spontaneous capacity to improve contractile performance. This reparative cytotype was characterized by high expression of homeobox transcription factor Nkx-2.5, T-box transcription factor TBX5, helix–loop–helix transcription factor MESP1, and myocyte enhancer factor MEF2C, markers of cardiopoiesis. Recombinant cardiogenic cocktail guidance secured the cardiopoietic phenotype across the patient cohort. Compared with unguided counterparts, cardiopoietic hMSC delivered into infarcted myocardium achieved superior functional and structural benefit without adverse side effects. Engraftment into murine hearts was associated with increased human-specific nuclear, sarcomeric, and gap junction content along with induction of myocardial cell cycle activity.

Conclusions Guided cardiopoiesis thus enhances the therapeutic benefit of bone marrow-derived hMSC in chronic ischemic cardiomyopathy. (J Am Coll Cardiol 2010;56:721–34) © 2010 by the American College of Cardiology Foundation

Cell-based reparative approaches are increasingly considered in the management of ischemic heart disease. Stem cell capacity for multilineage tissue specification provides the opportunity to extend treatment options for ischemic cardiomyopathy beyond current practices and achieve heart repair (1–3).

See page 735

Emerging experience has focused on adult stem cells delivered unaltered, in their native state (4,5). Of increased interest are mesenchymal stem cells with a documented aptitude for multipotent differentiation, cytoprotection, and myocardial restoration demonstrated when derived from allogeneic healthy donors (6–8). However, in autologous therapy, patient-related modifiers of regenerative capacity, including age, sex, and comorbidities, translate into variability in repair-compromising efficacy (9–11). Development of technologies that would enhance stem cell benefit is thus warranted (1–13).

From the *Department of Medicine, Division of Cardiovascular Diseases, Marriott Heart Disease Research Program, Mayo Clinic, Rochester, Minnesota; †Department of Physical Medicine and Rehabilitation, Mayo Clinic, Rochester, Minnesota; ‡Cardio3 BioSciences, Mont-Saint-Guibert, Belgium; and the §Cardiovascular Center, OLV Ziekenhuis, Aalst, Belgium. Supported by National Institutes of Health (grants #HL83439, #HL85208), American Heart Association, Marriott Heart Disease Research Program, Cardio3 BioSciences, Ted Nash Long Life Foundation, Ralph Wilson Medical Research Foundation, Mayo Clinic General Mills Clinician-Investigator Fellowship, Mayo Graduate School, Mayo Clinic FUTR Career Development Award, and Mayo Clinic Discovery Translation Program. Drs. Behfar, Gaussin, Homsy, Bartunek, and Terzic serve on the research advisory board of Cardio3 BioSciences.

Manuscript received August 24, 2009; revised manuscript received March 2, 2010, accepted March 9, 2010.

JACC Vol. 56, No. 9, 2010
August 24, 2010:721–34

Abbreviations and Acronyms

BMP = bone morphogenetic protein
DNA = deoxyribonucleic acid
FGF = fibroblast growth factor
GMP = good manufacturing practice
hMSC = human mesenchymal stem cell
IGF = insulin-like growth factor
IL = interleukin
mRNA = messenger ribonucleic acid
PCR = polymerase chain reaction
TGF = transforming growth factor

We here tracked interpatient variation in stem cell effectiveness and identified that expression of cardiac markers in human mesenchymal stem cells (hMSCs) biases repair. Accordingly, nonreparative hMSC were guided to acquire regenerative potency through cardiogenic priming. Derived cardiopoietic hMSC demonstrated improved efficacy compared with their naïve source, establishing an adult stem cell–derived progenitor with enhanced benefit in the treatment of chronic ischemic cardiomyopathy.

Methods

Study protocols were approved by pertinent institutional ethics committee, institutional review board, and institutional animal care and use committee.

Ischemic heart disease patient cohort. Patients undergoing coronary artery bypass surgery provided informed consent. Information concerning age, sex, history, medications, perioperative laboratory evaluation, and coronary assessment is presented in Online Tables 1 to 3.

Stem cell culture. Human bone marrow aspirates, obtained during coronary artery bypass surgery following sternotomy, yielded plastic-adherent hMSC with identity confirmed by fluorescence-activated cell sorting using the $CD34^-/CD45^-/CD105^+/CD133^+$ panel (Online Fig. 1). Cells were cultured at 37°C in advanced minimal essential medium supplemented with 5% human platelet lysate (14), and stimulated with transforming growth factor (TGF)-$beta_1$ (2.5 ng/ml), bone morphogenetic protein (BMP)-4 (5 ng/ml), activin A (5 ng/ml) (15,16), fibroblast growth factor (FGF)-2 (10 ng/ml) (6), interleukin (IL)-6 (100 ng/ml) (17), factor IIa (h-alpha-thrombin, 1 U/ml) (18), insulin-like growth factor (IGF)-1 (50 ng/ml) (6), and/or retinoic acid (1 μmol/l) (19). Phospho-Akt inhibition was achieved with SR13668 (50 nmol/l). Differentiation beyond the cardiopoietic state was carried out with 1% platelet lysate in the presence of FGF-2 and h-alpha-thrombin for 10 days. To scale-up production under good manufacturing practice (GMP) compliance, cell culture procedures were site-certified by independent regulatory review as meeting mandatory environmental and quality assurance criteria required to ensure traceability, purity, homogeneity, and sterility for batch testing and release (14).

Ribonucleic acid profiling. Real-time quantitative polymerase chain reaction (PCR) was performed using a TaqMan PCR kit (Applied BioSystems, Carlsbad, California) in triplicate. Threshold cycle (C_T) values were determined using the $2^{-\Delta\Delta C}{}_T$ method, normalized to human-specific *GAPDH* (TaqMan, Applied BioSystems). Genes representative of cardiac transcriptional activity included homeobox transcription factor Nkx-2.5 (Hs00231763_m1), GATA-4 (Hs00171403_m1), myocyte enhancer factor MEF2C (Hs00231149_m1), T-box transcription factor TBX5 (Hs00361155_m1), FOG-1 (Hs00542350_m1), helix-loop-helix transcription factor MESP1 (Hs00251489_m1), GATA-6 (Hs00232018_m1), and Flk-1 (Hs00911699_m1).

Protein and deoxyribonucleic acid probing. Immunostaining for cardiac transcription factors MEF2C (1:400, Cell Signaling Technologies, Danvers, Massachusetts), Nkx-2.5 (1:150, Santa Cruz Biotechnology, Santa Cruz, California), GATA-4 (1:150, Santa Cruz Biotechnology), TBX5 (1:5000, Abcam, Cambridge, Massachusetts), MESP1 (1:250, Novus Biologicals, Upplands Väsby, Sweden), FOG-2 (1:100, Santa Cruz Biotechnology), along with Phospho-Akt^{Ser473} (1:100, Cell Signaling Technologies), human-specific troponin I (1:100, Abcam), sarcomeric alpha-actinin (1:500, Sigma-Aldrich, St. Louis, Missouri), ventricular myosin light chain MLC-2V (1:500, Synaptic Systems, Goettingen, Germany), Sca-1 (1:100, R&D Systems, Minneapolis, Minnesota), CD-31/PECAM-1 (1:500, Beckman Coulter, Brea, California), alpha-smooth muscle actin (1:500, Sigma), human lamin A/C (1:50, Novocastra, Leica Microsystems, Bannockburn, Illinois), connexin 43 (1:100, Zymed Laboratories, San Francisco, California), and Ki-67 (1:500, NeoMarkers, Thermo Scientific, Fremont, California) was performed following fixation in 3% paraformaldehyde and permeabilization with 1% Triton X-100 (Sigma). Human Alu deoxyribonucleic acid (DNA) probing (BioGenex, San Ramon, California) required hybridization (85°C, 10 min) and incubation at 37°C overnight followed by antifluorescein green fluorescent protein–labeled secondary detection. For genomic probing, human and murine DNA were labeled in Vysis Spectrum Green or Orange deoxyuridine triphosphate (Abbott Molecular, Abbott Park, Illinois) via nick translation followed by hybridization and denaturation. Frozen tissue was fixed (3:1 methanol/acetic acid), and pre-treated in 2x SSC (15 mM sodium chloride + 1.5 mM sodium citrate × 2 H_2O) for 2 min (73°C), placed 5 min in 1 mol/l tris, 0.5 mol/l ethylenediamine tetraacetic acid (90°C), 2 min in 4 mg pepsin/l, 0.9% NaCl (37°C), and 30 s in 70% ethyl alcohol. Slides were denatured in 70% formamide (73°C), followed by a 70%/85%/100% ethyl alcohol series. Denatured genomic probes were applied to sections, hybridized overnight (37°C), and washed in 2x SSC/0.1% NP40 solution (73°C). Slides were counterstained with 4,6-diamino-2-phenylindole (DAPI)–containing mounting medium.

Cell imaging. Images were obtained with LSM 510/LSM 700 laser scanning confocal or ApoTome structured illumination microscopes (Carl Zeiss, Thornwood, New York). Quantification of cytosolic and nuclear induction of Nkx-2.5, MEF2C, or GATA-4 was performed using Zeiss Axioplan and MetaMorph software (Molecular Devices,

Sunnyvale, California). Cell cycle activity was quantified using a hematocytometer. Cell structure was resolved by transmission electron microscopy (20). Calcium transients were monitored in cells loaded with 5 μmol/l of the calcium-selective probe fluo-4-acetoxymethyl ester (Molecular Probes, Invitrogen, Carlsbad, California) using a temperature controlled Zeiss LSM 510 or ApoTome microscope with line-scan or phase images acquired during 1-Hz stimulation (15).

Cell therapy. Myocardial infarction was performed in 8 to 12 weeks old nude, immunocompromised mice (Harlan Laboratories, Indianapolis, Indiana) (21). Following intubation and ventilation under isoflurane anesthesia, proximal left anterior descending artery was ligated with 9-0 suture. Injury induced ST-segment changes on electrocardiography (MP150, Biopac, Goleta, California) and akinetic regions on echocardiography (Sequoia 512, Siemens, Munich, Germany; Vevo2100, VisualSonics, Toronto, Ontario). Following a blinded design, 1-month post-infarction hMSC (a total of 600,000), suspended in 12.5 μl phosphate buffered saline, were injected under microscopic visualization in 5 epicardial sites (120,000 cells per site) in the anterior wall of the left ventricle. A saline-treated group underwent an identical procedure. Left ventricular function and structure were serially followed by echocardiography at pre-infarction; 1-month after infarction (pre-cell therapy); and 1, 2, 6, 12, and 20 months post-cell therapy. Ejection fraction (%) was calculated as: $[(LVVd - LVVs)/LVVd] \times 100$, where LVVd is left ventricular end-diastolic volume (μl), and LVVs is left ventricular end-systolic volume (μl).

Statistics. Data are presented as mean ± SD unless otherwise indicated (JMP 8, SAS Institute, Cary, North Carolina). Paired group analysis was performed using Student *t* test for each pair of samples without correction for type I error, and nonparametrically validated using Wilcoxon signed rank test (JMP 8). Kaplan-Meier analysis with log-rank testing was applied for survival evaluation. A p value <0.05 was considered significant.

Results

Reparative profile extracted from patient stem cells demonstrating innate efficacy. Bone marrow-derived hMSC obtained from patients undergoing coronary artery bypass revealed individuals with an innate capacity for heart repair. Specifically, hMSC derived from 2 of 11 individuals significantly improved ejection fraction following myocardial injection into a nude murine model of chronic ischemic cardiomyopathy (Fig. 1A). No clinical features separating these patients from the cohort were apparent (Online Tables 1 to 3). Reparative stem cells were distinguished from noneffective hMSC counterparts by robust expression of early (homeobox transcription factor Nkx-2.5 [22], T-box transcription factor TBX5 [23], and the helix–loop–helix transcription factor MESP1 [24]) and late (myocyte enhancer factor MEF2C [25]) cardiac transcription factors (Fig. 1B). Distinctive protein abundance was corroborated on quantitative PCR with a 3- to 6-fold up-regulation in TBX5 and MESP1 and a 2- to 3-fold up-regulation of MEF2C messenger ribonucleic acid (mRNA) in effective versus noneffective hMSC, respectively (Fig. 1C). Up-regulated cardiac transcription factors in hMSC thereby provided a molecular signature consistent with ejection fraction improvement.

Induction of cardiac program in hMSC. To impose expression and potentiation of cardiac transcription factors, while maintaining proliferative status, endoderm-based pathways (26,27) contributing to embryonic cardiogenesis (15,16) were tested on the adult hMSC phenotype (Fig. 2). The TGF-beta superfamily members (TGF-$beta_1$, BMP-4, and activin-A), which induce Nkx-2.5 expression in embryonic stem cells (16), here individually promoted cytosolic Nkx-2.5 and MEF2C expression at protein (Fig. 2A, Online Fig. 2A) and mRNA (Online Fig. 2B) levels. Stimulation of hMSC with a combination of TGF-$beta_1$, BMP-4, and activin-A resulted in augmented Nkx-2.5 and MEF2C cytosolic expression, further enhanced by retinoic acid (Fig. 2A, Online Fig. 3). The TGF-beta superfamily members and retinoic acid did not achieve nuclear translocation of cardiac transcription factors, maintaining nuclear to cytosol ratios equivalent to untreated hMSC (Fig. 2B, first and second columns). Potentiation of cardiac transcription factors was achieved with IGF-1 and FGF-2 whose combination triggered nuclear translocation of Nkx-2.5 and MEF2C (Fig. 2B, fifth column, Online Fig. 4), correlating with Akt activation (Online Fig. 5) as nuclear expression was abolished by the Akt inhibitor, SR13668 (Fig. 2B, sixth column, Online Fig. 6). Stimulation of hMSC with TGF-$beta_1$, BMP-4, activin-A, retinoic acid, FGF-2, and IGF-1 (Fig. 2C, Passage 0) compromised cell proliferation, rescued by alpha-thrombin and IL-6 (Fig. 2C). Applied as a human recombinant cardiogenic cocktail, within a 5% platelet lysate at the onset of a 5-day incubation period, TGF-$beta_1$, BMP-4, activin-A, retinoic acid, FGF-2, IGF-1, alpha-thrombin, and IL-6 induced cardiac transcription factor expression, potentiated nuclear translocation, and maintained cell cycle progression (Fig. 2D). Induction of procardiogenic transcription factors was chronicled with mRNA profiling during and after cocktail exposure (Fig. 2E), and the derived cardiopoietic profile stabilized within 5 days was maintained for 7 passages.

Cardiogenic cocktail guides cardiopoiesis to yield functional cardiomyocytes. Guidance with the cardiogenic cocktail induced nuclear translocation of cardiac transcription factors, documented for Nkx-2.5 (86 ± 10% of cells), MEF2C (84 ± 8%), FOG-2 (78 ± 15%), TBX5 (76 ± 7%), MESP1 (83 ± 11%), and GATA-4 (81 ± 3%) (5,15,25,28), augmenting baseline expression limited to the cytosol in unguided hMSC (Fig. 3A). In this way, hMSC from each patient (n = 12) were guided to derive a cardiopoietic phenotype with nuclear up-regulation of cardiac transcription factors in the absence of sarcomere protein expression (Online Fig. 7A). This lineage engagement was further

JACC Vol. 56, No. 9, 2010
August 24, 2010:721–34

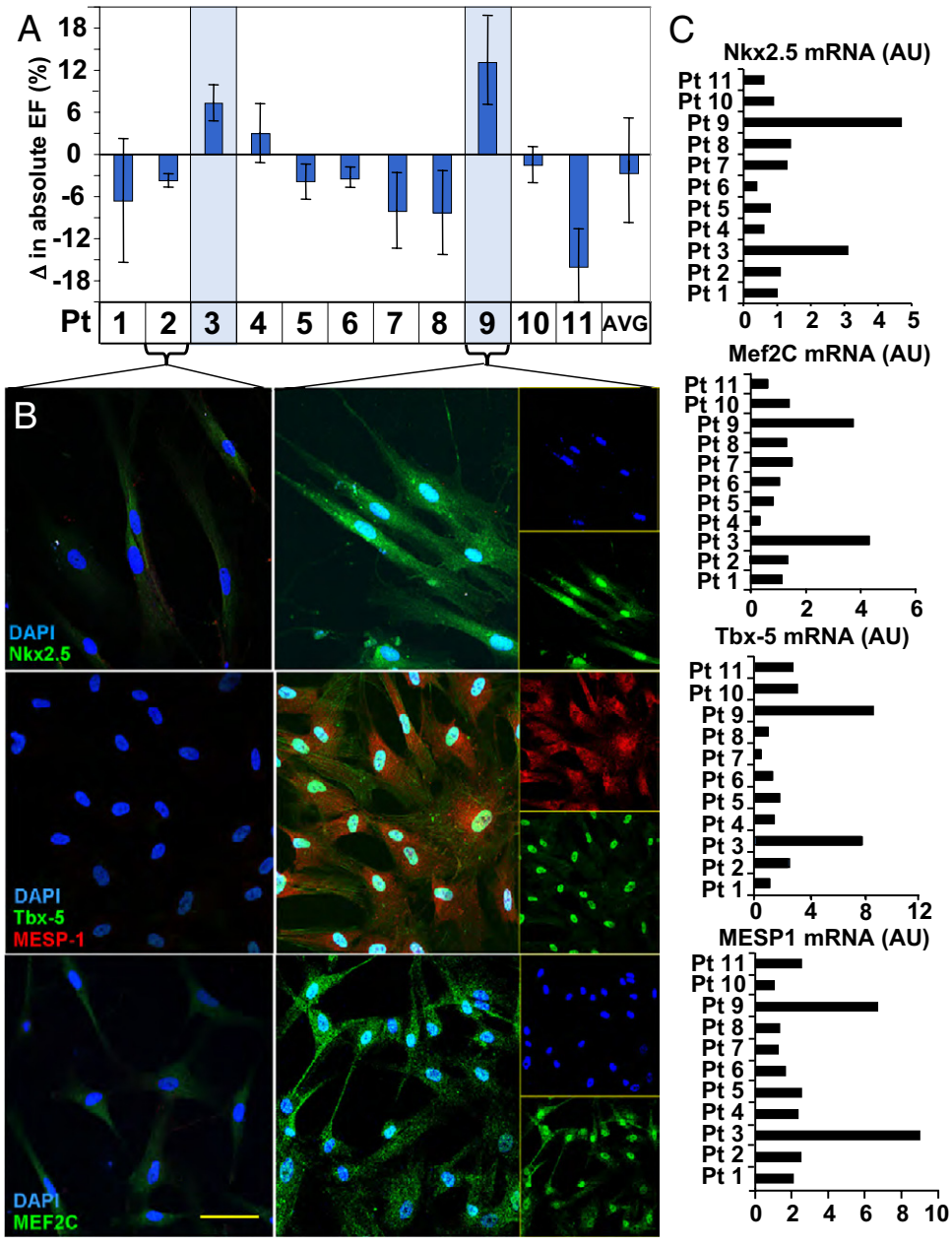

Figure 1 **Repair Efficacy in hMSC Correlates With Cardiac Transcription Factor Expression**

(A) Patient (Pt) = human mesenchymal stem cells demonstrated variable repair after injection into an infarction model. Only rare stem cells (Patients #3 and #9 highlighted) demonstrated benefit. **(B)** Low expression of cardiac transcription factors in nonreparative = human mesenchymal stem cells (hMSC) (Patient #2 illustrated). Robust Nkx-2.5 (83 ± 5% and 86 ± 2% of = hMSC in Patients #3 and #9), MEF2C, TBX5, and MESP1 expression in = hMSC with reparative capacity (Patient #9 shown, with single channels provided in **inset**). **Bar**: 20 μm. **(C)** Reparative pattern validated with up-regulated Nkx-2.5, MEF2C, TBX5, and MESP1 messenger ribonucleic acid (mRNA) in reparative versus nonreparative hMSC. AU = arbitrary units; AVG = average; DAPI = 4,6-diamino-2-phenylindole; EF = ejection fraction.

documented with mRNA analysis revealing a 12-, 16-, 6-, and 2-fold increase in Nkx-2.5, Flk-1, GATA-6, and FOG-1, respectively in treated versus untreated hMSC (Fig. 3B). Thereby, hMSC from patients with ischemic heart disease were converted in vitro from a naïve state of sequestered plasticity to active tissue specification adopting a phenotype consistent with enhanced repair aptitude.

Differentiation beyond the cardiopoietic state, in 1% human platelet lysate medium, ultimately achieved sarcomerogenesis tracked by expression of alpha-actinin (48 ± 10% of cells at Day 10 and 75 ± 8% at Day 15) and troponin I (75 ± 6% of cells at Day 10 and 86 ± 5% at Day 15), which demonstrated immature organization at 20-days post-cocktail stimulation (Fig. 3C, Online Fig. 7B). Smooth

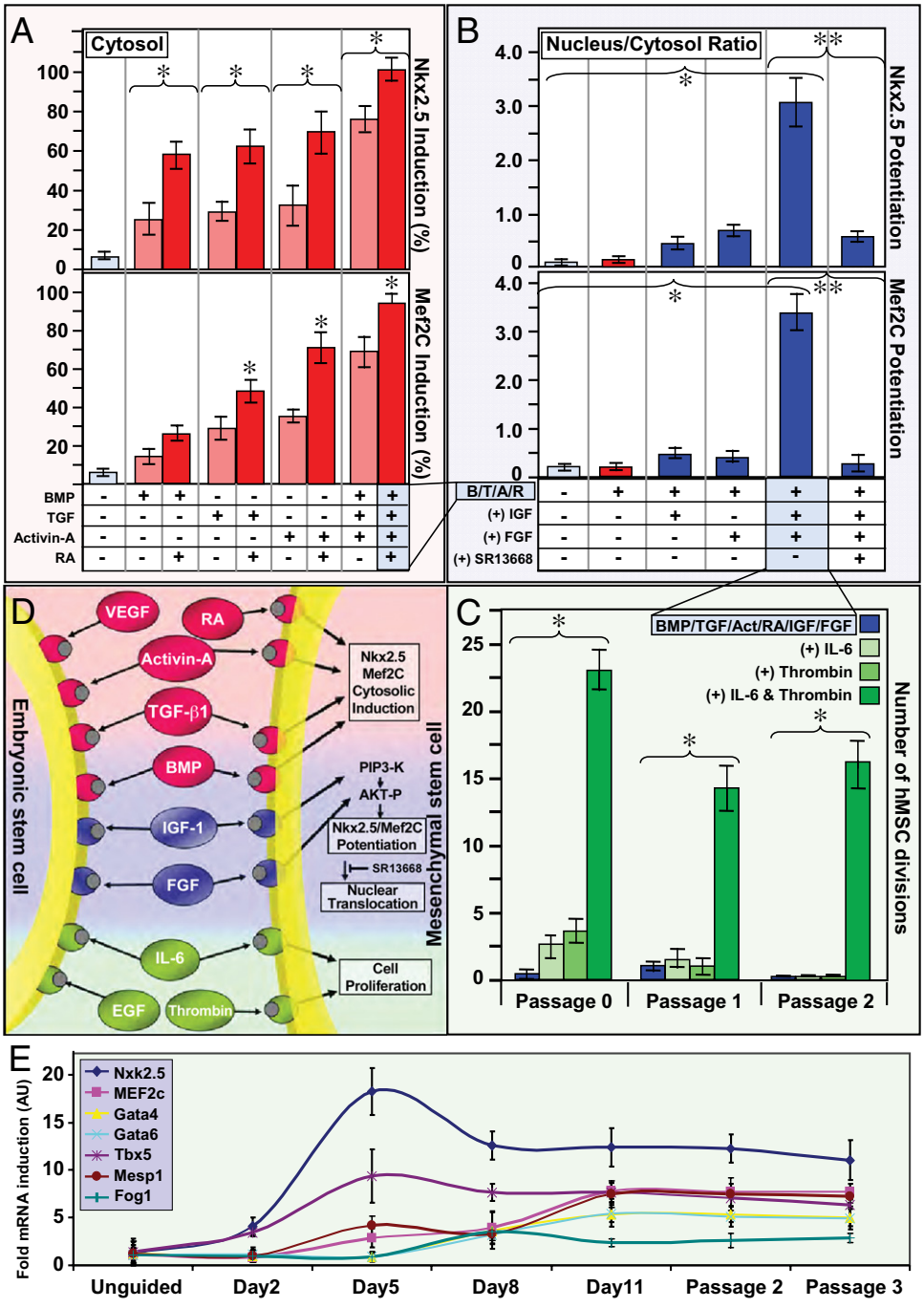

Figure 2 **Derivation of Cardiogenic Cocktail That Induces and Potentiates Cardiac Transcription Factor Expression and Maintains Cell Cycle Activity**

(A) Bone morphogenetic protein (BMP)-4, transforming growth factor (TGF)-beta$_1$, and activin-A induced cytosolic expression of Nkx-2.5 and MEF2C **(light red)**. Addition of retinoic acid (RA) boosted cytosolic induction **(red)**. **(B)** BMP-4, TGF-beta$_1$, activin-A, and RA **(red)** potentiated nuclear translocation of Nkx-2.5 and MEF2C when combined with insulin-like growth factor (IGF)-1 and fibroblast growth factor (FGF)-2. Akt inhibitor (SR13668) inhibited nuclear translocation. **(C)** Low hMSC cell cycle activity following BMP-4, TGF-beta$_1$, activin-A, retinoic acid, IGF-1, and FGF-2 treatment **(blue)** rescued by interleukin (IL)-6 and human alpha-thrombin. **Brackets** indicate pared analysis. **Star** and **double star:** $p < 0.05$. **(D)** Cardiogenic cocktail, applied as a combined regimen, induced and potentiated nuclear translocation of Nkx-2.5 and MEF2C while maintaining cell cycle activity. **(E)** Nkx-2.5, TBX5, MEF2C, GATA-4, GATA-6, FOG-1, and MESP1 hMSC mRNA in response to cocktail treatment. **A to C** and **E** evaluate nonreparative patient hMSC. B/T/A/R = bone morphogenetic protein-4, transforming growth factor-beta$_1$, activin-A, and retinoic acid; EGF = epidermal growth factor; VEGF = vascular endothelial growth factor; other abbreviations as in Figure 1.

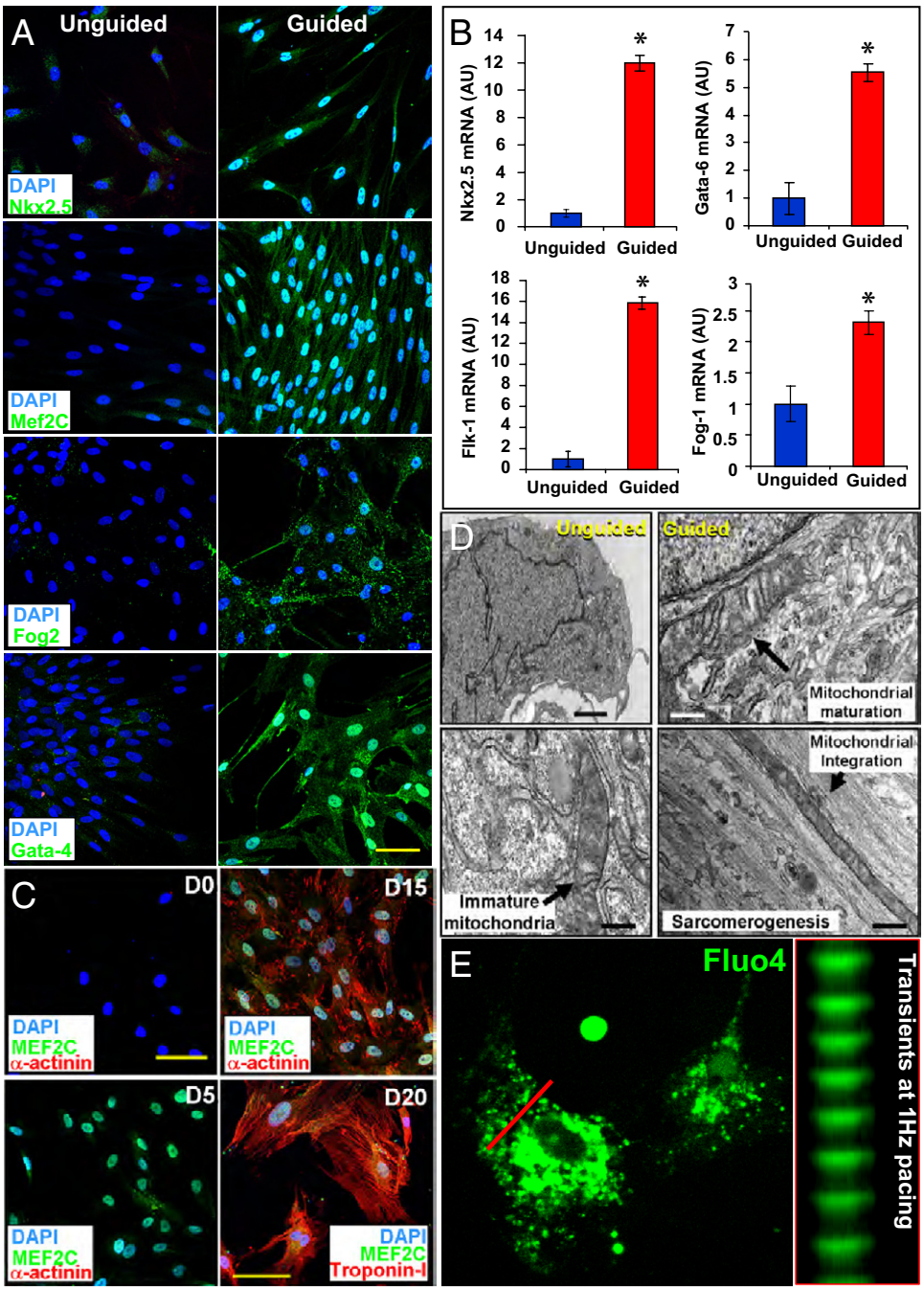

Figure 3 Cardiogenic Cocktail Guides Cardiogenesis to Yield Functional Cardiomyocytes

(A) Nuclear translocation of Nkx-2.5, MEF2C, FOG-2, and GATA-4 in cocktail-guided hMSC. **(B)** Guidance of hMSC, from 12 coronary artery disease patients, increased mRNA expression of Nkx-2.5, Flk-1, GATA-6, and FOG-1. **Star:** $p < 0.01$. **(C)** Cocktail-based cardiogenic conversion of naïve hMSC (D0) resulted in MEF2C activation at Day 5 (D5) and sarcomerogenesis (alpha-actinin) achieved by Days 15 (D15) to 20 (D20, troponin I expression). **Bar:** 20 μm. **(D)** Compared with naïve hMSC with abundant nuclei **(left)**, transmission electron microscopy of cocktail-guided hMSC at Day 15 revealed mitochondrial maturation and integration with organizing myofibrils. **Bar:** 1 μm **(upper left)**; 250 nm **(other 3 panels)**. **(E)** Calcium transients elicited in response to 1-Hz electrical stimulation (Online Video 5). Abbreviations as in Figure 1.

muscle actin stained myocytes were rarely observed (1 ± 1% of cells) at Day 20 of differentiation (Online Fig. 7B). Nascent cardiomyocytes derived from guided hMSC contained ~80% of mitochondria with structured cristae and aligned with forming sarcomeres, in contrast to unguided hMSC characterized by prominent nuclei and immature mitochondria (Fig. 3D, Online Fig. 7C). At Day 20 (15 days after the end of cocktail stimulation), functional excitation-contraction coupling was documented by rhythmic calcium transients in fluo-4 loaded cells seen in re-

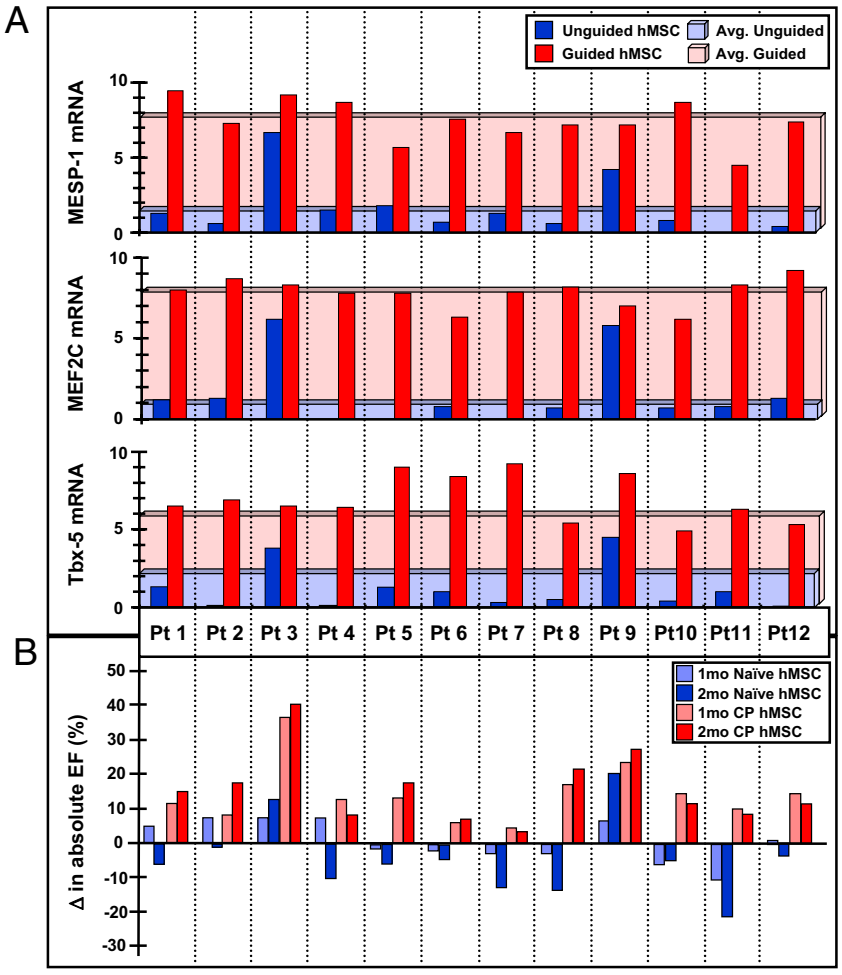

Figure 4 **Cardiopoietic hMSC Phenotype Associated With Ejection Fraction Improvement**

(A) Induction of cardiac transcription factors TBX5, MEF2C, and MESP1 mRNA documented for each patient. **(B)** Echocardiography demonstrated ejection fraction improvement in chronically infarcted mice treated with cardiopoietic over patient-matched naïve hMSC at 1 to 2 months. Experiment in **B** distinct from Figure 1A. CP = cardiopoietic; other abbreviations as in Figure 1.

sponse to external electrical stimulation (Fig. 3E, Online Videos). Thus, the cardiopoietic phenotype derived from hMSC can yield sarcomere-containing myocytes capable of electromechanical response.

Cardiopoietic guidance enhances therapeutic efficacy of hMSC. Guided hMSC (n = 12) demonstrated on average a 3-fold increase in TBX5 and an 8-fold increase in MESP1 and MEF2C (Fig. 4A). Induction of the cardiopoietic phenotype was verified with real-time quantitative PCR prior to transplantation into nude mice 1 month after coronary ligation. Permanent ligation of the left anterior descending artery induced akinesis and dyskinesis in the anterior wall (ejection fraction: 78.8 ± 2.1% and 38.2 ± 1.2%, pre- vs. post-infarction, $p < 0.05$) with an 84.6% survivorship at 1 month (n = 52). Surviving infarcted mice were randomized into saline-, naïve hMSC-, and cardiopoietic hMSC-treatment groups. Direct myocardial delivery of cardiopoietic hMSC, demonstrating nuclear translocation of cardiac transcription factors in the absence of sarcomeric proteins, was used to eliminate variability introduced by reliance on distal homing. Despite equivalent akinesis (saline: 31.3 ± 2.6%, naïve hMSC: 33.1 ± 2.6%, cardiopoietic hMSC: 35.3 ± 2.3%), guided cardiopoietic hMSC improved ejection fraction over patient-matched naïve hMSC at 1 and 2 months after transplantation (Fig. 4B). Echocardiography of cardiopoietic hMSC-treated chronically infarcted mice (n = 14, typically 1 mouse per patient) revealed progressive reanimation of the anterior left ventricular wall on 1-year follow-up (Fig. 5A, Online Videos), compared with marginal change recorded with patient-matched naïve hMSC (n = 17 mice) (Fig. 5A, left panels) or saline (n = 10 mice). Across cohorts, cardiopoietic hMSC were superior throughout 12 months for preventing heart failure progression (Fig. 5B). Relative to saline-treated hearts, cardiopoietic hMSC demonstrated sustained benefit superior to naïve therapy (Fig. 5C), result-

JACC Vol. 56, No. 9, 2010
August 24, 2010:721–34

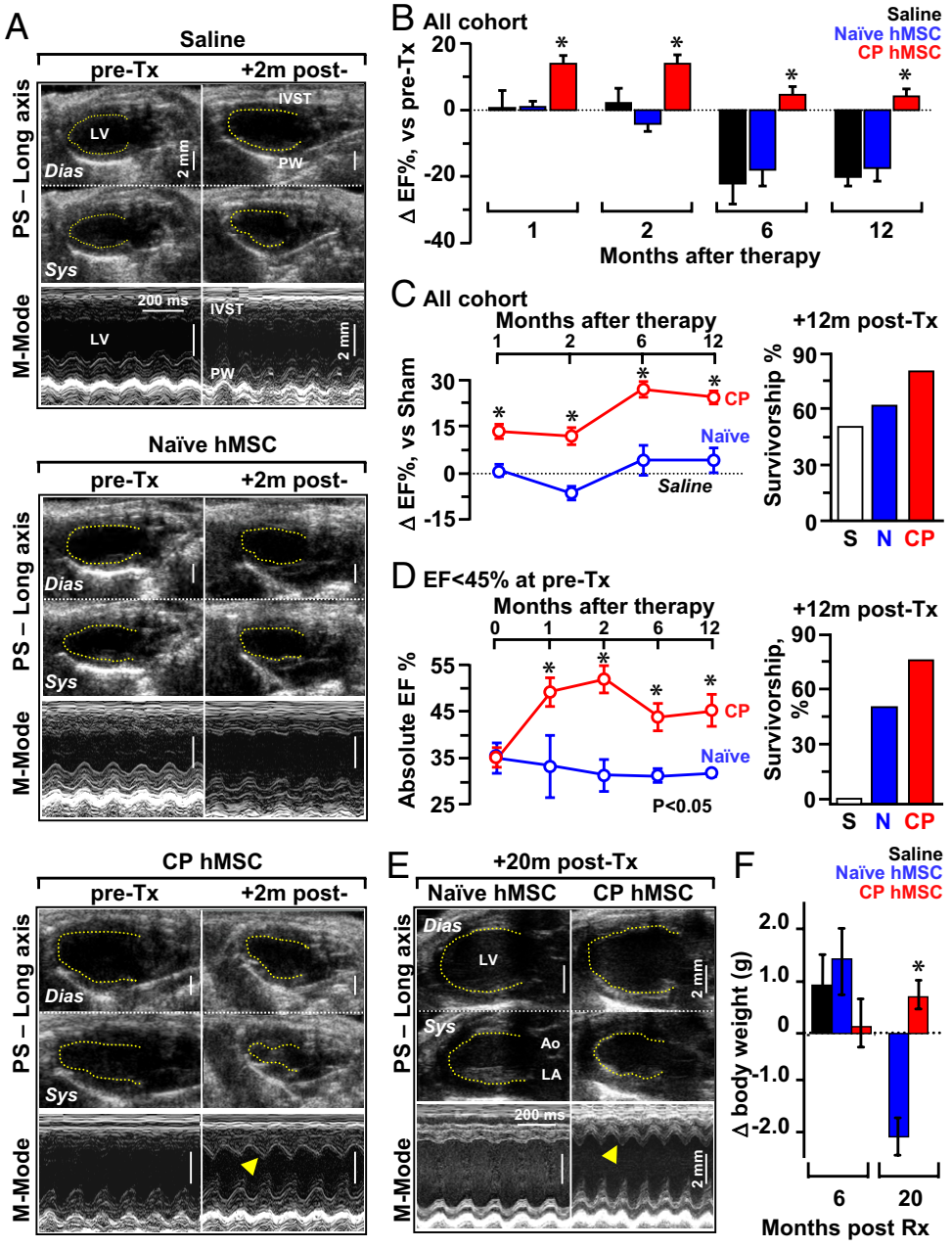

Figure 5 Cardiopoietic hMSC Provide Benefit Following Transplantation

(A) Echocardiography of infarcted hearts 4 weeks after coronary ligation, prior to therapy revealed an akinetic anterior wall. Saline and naïve hMSC-treated hearts maintained akinesis in the anterior wall, in contrast to reanimation in cardiopoietic treated (+2 months after therapy, **arrowhead**). See Online Videos 1 and 2 [Patient 11 naïve Rx 1 year] and Online Videos 3 and 4 [Patient 11 CP Rx 1 year]. **(B)** Cardiopoietic transplantation (n = 14) was associated with ejection fraction improvement acutely and limited progression toward failure chronically, not observed in saline (n = 10) or naïve groups (n = 17). **(C)** Sustained benefit of cardiopoietic hMSC therapy over 1-year follow-up, compared with naïve hMSC treatment, was associated with survival benefit **(right)**. Ejection fraction expressed relative to sham **(dotted line)**. **(D)** Subgroup analysis of mice with heart failure (pre-therapy ejection fraction <45%), cardiopoietic hMSC treatment had superior benefits versus naïve, with maintained survival **(right)**. Saline-treated mice in this subgroup did not survive beyond 2 months. **(E,F)** Cardiopoietic hMSC treatment prevented heart failure and blunted weight loss, compared with naïve (n = 5) at 20 months. In **E**, **arrowhead** indicates reanimated anterior wall. **Error bars** represent SEM. **Star**: $p < 0.01$ in **B, C,** and **D**; $p < 0.05$ in **F**. Ao = aorta; Dias = diastole; LA = left atrium; LV = left ventricle; N = naïve group; post-Tx = after therapy; pre-Tx = prior to therapy; S = saline group; Sys = systole; other abbreviations as in Figures 1 and 4.

ing in a 1-year survival of 78% and 61%, respectively, versus 48% for the saline-treated cohort (Fig. 5C inset). The benefit of cardiopoietic hMSC was particularly prominent in the subgroup with ejection fraction <45% (Fig. 5D) resulting in 1-year survival of 75% in contrast to 48% for naïve and 0% for saline-treated counterparts. Naïve hMSC

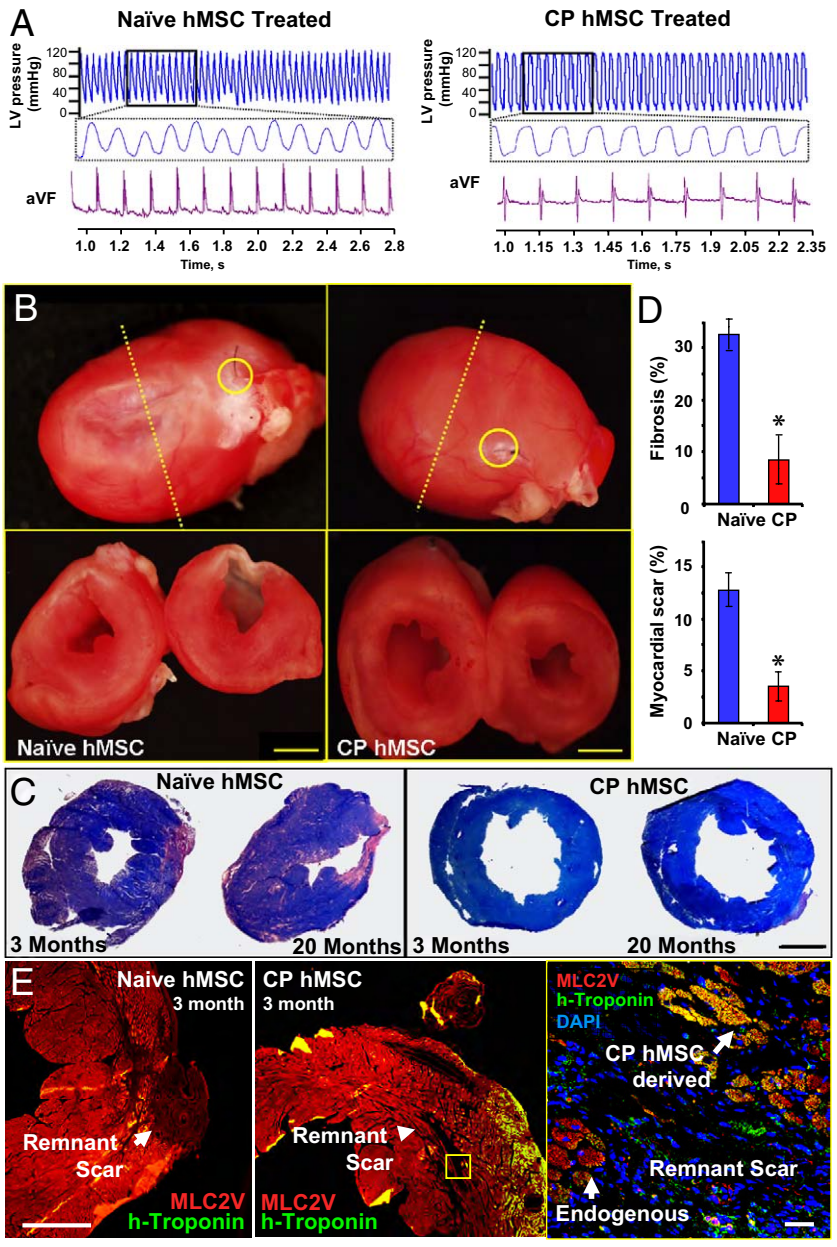

Figure 6 **Echocardiographic Improvement Validated With Pressure Catheter and Histopathological Evaluation**

(A) Catheterization revealed no afterload discrepancy between cohorts, yet elevated end-diastolic pressures were noted in naïve versus cardiopoietic hMSC groups. **(B)** Pathological evaluation demonstrated diminished scar downstream of left anterior descending artery ligation **(yellow circle)** with remuscularization and diminished remodeling in cardiopoietic **(right)** in contrast to naïve **(left)** treated hearts at 3 months **(yellow circle)**. **(C)** Diffuse fibrosis and larger scar area at 3 and 20 months in naïve compared with cardiopoietic hMSC-treated hearts. **Bar:** 2 mm for **B** and **C**. **(D)** Scar size and total myocardial fibrosis ($n = 10$ per condition). **Star:** $p < 0.01$. **(E)** Immunohistological evaluation of scar reveals limited contribution of human troponin cells in naïve **(left)** in contrast to cardiopoietic-treated hearts **(middle, right)**. **Bar:** 500 μm **(left)** and 20 μm **(right)**. MLC2V = ventricular myosin light chain; other abbreviations as in Figures 1, 4, and 5.

demonstrated limited capacity for recovery (Fig. 5D) with myocardial dysfunction (Fig. 5E), and cachexia observed at 20-month follow-up was typically absent from the cardiopoietic hMSC-treated group (Fig. 5F). Distinct outcomes were corroborated with cardiac catheterization that revealed abnormal end-diastolic pressure increase in the naïve hMSC-treated group, absent from cardiopoietic hMSC-treated mice despite equivalent afterload pressure profiles (Fig. 6A). Histopathology revealed progressive scar formation in naïve hMSC-treated hearts, attenuated with cardiopoietic hMSC treatment over 3 to 20 months (Figs. 6B and 6C, Online Fig. 8A). Global myocardial fibrosis and scar size were 32 ± 4% and 12 ± 2% in naïve hMSC-treated hearts versus 8 ± 6% and 3 ± 2% in cardiopoietic

hMSC-treated hearts ($n = 10$ for each group, $p < 0.01$), respectively (Fig. 6D). In contrast to persistent scar and low human-troponin staining in the naïve hMSC group, the anterior wall of cardiopoietic hMSC-treated hearts revealed human-specific troponin positive cardiomyocytes (Fig. 6E, Online Figs. 8B and 8C). Thus, treatment with cardiopoietic hMSC resulted in stable functional and structural benefits in chronically infarcted hearts.

Delivery of cardiopoietic hMSC triggers safe repair. Histological evaluation of murine hearts 48 h after delivery of fluorochrome-loaded cardiopoietic hMSC-validated epicardial delivery demonstrating cellular implantation (Fig. 7A). The hMSC engraftment within treated myocardium, quantified utilizing a human-specific *GAPDH* standard curve derived from murine hearts treated with escalating doses of hMSC (Fig. 7B), was 3.3 ± 2.8% and 3.4 ± 0.7% of cells injected for naïve, and 13.8 ± 2.4% and 9.6 ± 1.2% of cells injected for cardiopoietic hMSC at 3 months and 2 years, respectively (Fig. 7C). Cardiopoietic hMSC-treated murine myocardium revealed widespread presence of human-derived cells with positive staining for Alu-DNA sequences specific to the human species; the human-derived cells were absent in saline-treated infarcted controls (Fig. 7D). Quantification of human lamin within the infarcted anterior wall, validated with Alu-DNA staining, revealed 3 ± 2% ($n = 5$) versus 25 ± 5% ($n = 5$) of nuclei in naïve and cardiopoietic hMSC-treated hearts, respectively ($p < 0.01$). Typically, nuclear fusion was absent in cardiopoietic hMSC-treated hearts as determined by species-specific DNA hybridization, albeit cytosolic fusion could not be ruled out (Fig. 7E; see rare event in Online Fig. 9A). Cardiopoietic hMSC-derived human lamin–positive myocytes integrated with host tissue as demonstrated by colocalization with connexin-43, a gap junction protein (Fig. 7F). Cardiopoietic hMSC transplantation was thus associated with long-term cellular retention and nonfusogenic integration within the myocardium. Engrafted cardiopoietic hMSC displayed a ventricular phenotype as counterstaining of human troponin-positive cells colocalized with ventricular myosin light chain (MLC-2V) in the resolving scar (Fig. 8A, Online Fig. 8B). Within the anterior wall of cardiopoietic hMSC-treated hearts, colocalization of human cardiac troponin I with alpha-actinin (Fig. 8B, Online Fig. 8C) accounted for 12 ± 3% of cardiomyocytes, in contrast to 2.5 ± 2% of naïve hMSC-treated hearts (Figs. 8B and 8F). Furthermore, human-troponin–positive cardiomyocytes and adjacent murine myocardium in cardiopoietic hMSC-treated hearts had a significantly higher expression of Ki-67 (35 ± 3%) compared with naïve hMSC-treated heart (10 ± 5%), indicative of cell cycle engagement of endogenous and hMSC-derived cardiomyocytes up to 3 months after delivery (Figs. 8B and 8F). Specifically in the cardiopoietic hMSC-treated myocardium, 10 ± 3% of human troponin and 3 ± 2% of nonhuman alpha-actinin/MLC-2V positive cardiomyocytes expressed Ki-67. In addition, nonhuman Sca-1 cells were induced from 5.1 ± 3 to 18.6 ± 5.7 cells per field in naïve versus cardiopoietic hMSC-treated hearts (Online Figs. 9B and 9C) (29). Cardiopoietic hMSC-treated myocardium demonstrated vasculogenic potential, observed distal to the occluded coronary vessel with expression of human PECAM-1 (CD-31) (Figs. 8D and 8G) and colocalization of human lamin with alpha-smooth muscle actin (Figs. 8E and 8H). As such, transplanted cardiopoietic hMSC contributed to the myocardial pool, up-regulated cell cycle activity, induced endogenous Sca-1-positive stem cell proliferation, and contributed to neovasculogenesis distal to the site of ligation. Long-term safety of cardiopoietic hMSC was documented by absence of myocardial tumorigenesis (Online Fig. 10A) or electrical ectopy on electrocardiography (Online Fig. 10B). Beyond the heart, at 1-year follow-up, no evidence of abnormal cell proliferation or neoplastic transformation was found on gross or histological examination of other well-perfused organs (Online Fig. 10C). Thus, transplantation of cardiopoietic hMSC achieved lineage specification for safe repair in the setting of ischemic cardiomyopathy.

Scaled-up GMP production of cardiopoietic hMSC. Following safety and efficacy testing, the feasibility of scaled-up cardiopoietic hMSC production under GMP criteria was evaluated (7,14). With regulatory approval, cardiopoietic guidance was carried out using standard operating procedures with each cocktail component adhering to GMP guidelines. In this way, ≥600 million cardiopoietic hMSC were derived within 6 weeks of patient bone marrow harvest meeting sterility, purity, and homogeneity release criteria. The GMP-grade cardiopoietic hMSC were successfully derived from 10 patients and released following demonstration of cardiac transcription factor up-regulation consistent with an aptitude for repair. Thus, guided cardiopoiesis under GMP stringency demonstrated the capacity for scalable manufacturing of a stem cell biologics with imposed cardioreparative traits.

Discussion

Heterogeneous outcome among patients treated with autologous stem cells is recognized as an impediment to broader clinical acceptance of cell-based therapy in cardiovascular medicine (5,9,11,30,31). The present study identified individuals that harbored hMSC with an innate capacity for myocardial repair. Reparative stem cells were characterized by up-regulation of cardiac transcription factors, suggesting that pre-emptive cardiogenic specification could ensure enhanced therapeutic efficacy of hMSC.

Indeed, hMSC are a desirable source for organ repair due to accessibility for harvest, propensity to propagate in culture, and favorable biological profile (32,33). Discovered as a byproduct of hematopoietic stem cell isolation, derivation of hMSC is confounded, however, by phenotype heterogeneity among patients compromising therapeutic efficacy (34). Here, evaluation of adult stem cells with innate reparative potential identified traits associated with regenerative efficacy, consistent with expression of early and late

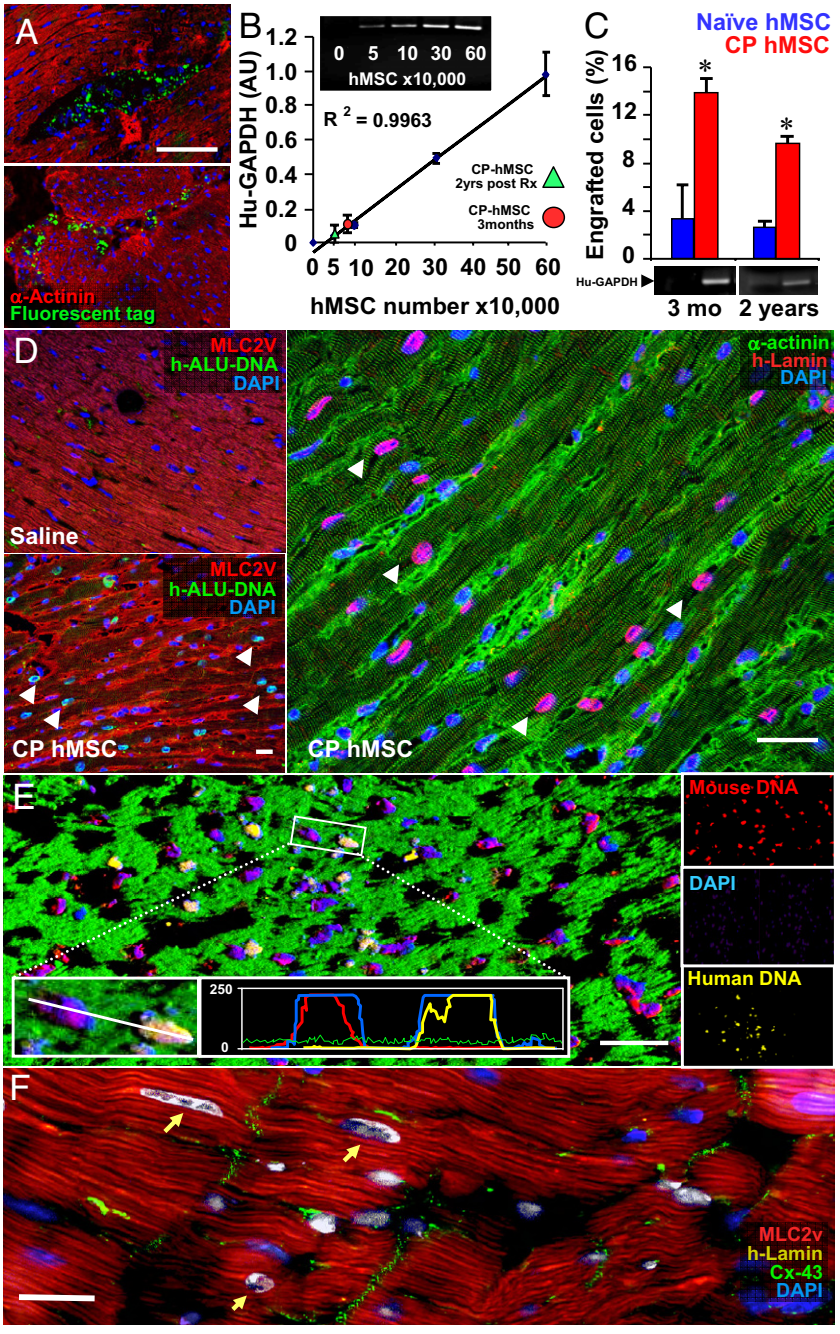

Figure 7 **Cardiopoietic hMSC Demonstrate Long-Term Integration**

(A) Fluorochrome-loaded cardiopoietic human mesenchymal stem cells detected within murine myocardium 48 h after delivery. **(B)** mRNA standard curve for human-specific *GAPDH* with escalating doses of hMSC within murine myocardium. Quantified hMSC engraftment (3 months, **red circle**; 2 years, **green triangle**). **(C)** Higher cardiopoietic hMSC engraftment when compared with naïve group. **Star:** $p < 0.01$. **(D)** Compared with saline group **(left)**, cardiopoietic hMSC within treated hearts confirmed by human Alu deoxyribonucleic acid **(green, middle)** and immunoprobing for human-specific lamin **(red, right)**. **(E)** Concurrent human **(yellow)** and mouse **(red)** deoxyribonucleic acid–probing demonstrated negligible fusion through species-specific nuclear staining on confocal histogram and single-channel analysis **(insets)**. **Bar:** 20 μm for **A, D,** and **E**. **(F)** Human lamin **(yellow, arrows)** expressing myocytes demonstrated connexin 43 **(green)** expression. **Bar:** 10 μm. Cx = connexin; h-Alu-DNA = human Alu deoxyribonucleic acid; other abbreviations as in Figures 1, 4, and 6.

cardiac transcription factors (15,25,35). Although expression of cardiac transcription factors is also seen in embryonic stem cells and is pivotal in their response to a natural sequence and duration of cardiogenic stimuli, the pluripotent phenotype has the distinctive capacity to readily engage into a program of lineage specification with orchestrated and targeted signaling driving cardiac differentiation (15,26,36,37). In contrast, adult stem cells demonstrate a

JACC Vol. 56, No. 9, 2010
August 24, 2010:721–34

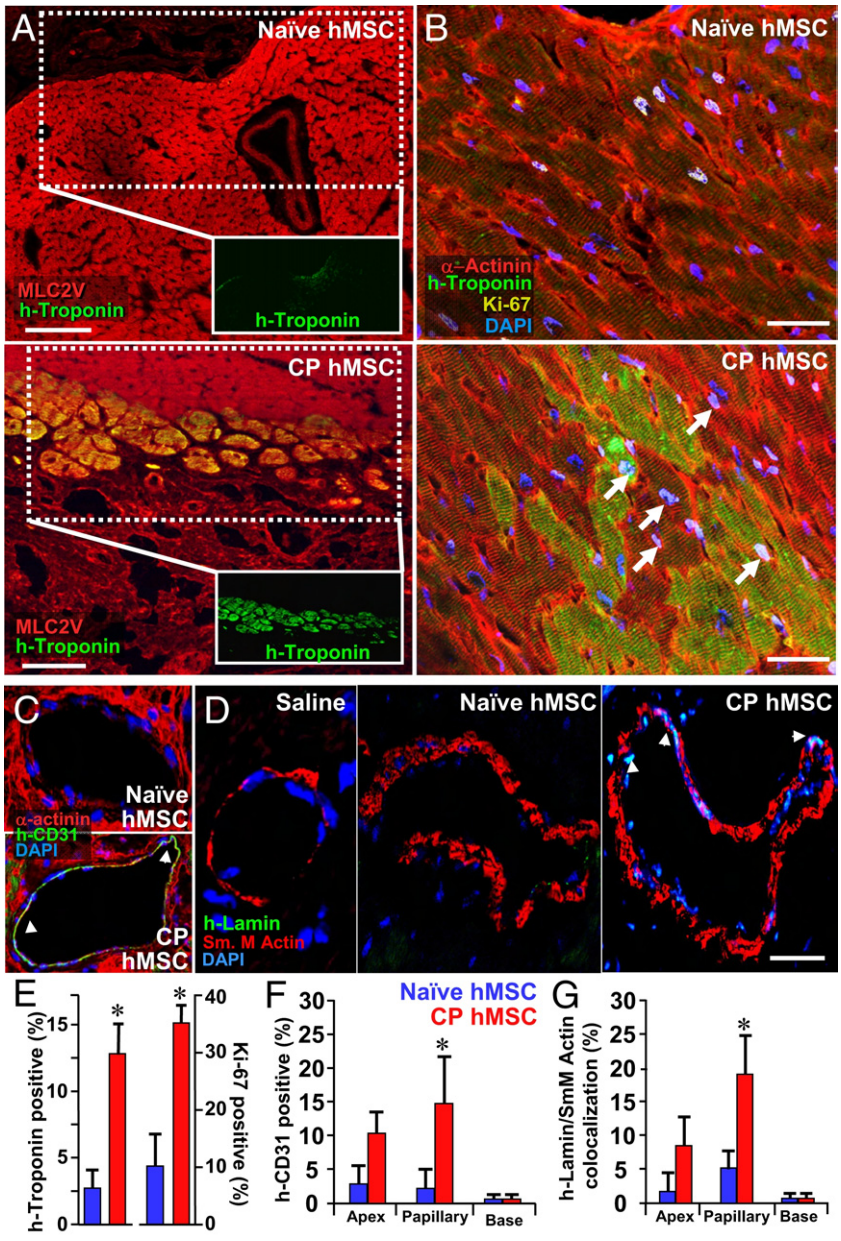

Figure 8 **Cardiopoietic hMSC Demonstrate Cardiogenic and Vasculogenic Potential Within Host Myocardium**

(A) Human-specific troponin I **(green)** in the anterior wall of naive- versus cardiopoietic-treated hearts, respectively, colocalized with MLC2V (**red**). **Bar:** 100 μm. **(B)** Human troponin I staining of naïve versus cardiopoietic hMSC-treated hearts, counterstained with alpha-actinin **(red)**, demonstrated engraftment of human cells. Cell cycle activation, documented by Ki-67 expression **(yellow, arrows)**, noted in human troponin positive and endogenous cardiomyocytes. **(C)** Confocal evaluation of collateral vessels from cardiopoietic hMSC-treated hearts demonstrated human-specific CD-31 (PECAM-1) staining. **(D)** Human lamin staining **(arrows)** colocalized with nuclei of smooth muscle in vessels from cardiopoietic hMSC-treated but not saline- or naïve-treated hearts. **Bar:** 20 μm for **B to D**. **(E)** Percentage of human troponin and Ki-67 positive cells in myocardial wall, up-regulated in cardiopoietic versus naïve hMSC-treated hearts (n = 10). **(F,G)** Quantification of human CD-31 and colocalization between human lamin and smooth muscle actin reveals significant contribution at the level of the papillary muscle from cardiopoietic hMSC group compared with naïve group (n = 10 in **F** and **G**). **Star:** $p < 0.05$. Abbreviations as in Figures 1, 4, and 6.

latent plasticity, unmasked within strongly conducive in vivo environments to yield tissues emanating from all germinal layers (38–40). In vitro, adult stem cells demonstrate a limited capacity for differentiation, requiring protracted and continuous growth factor exposure to trigger cell fate specification (30,38). In this study, a combinatorial application of a set of recombinant factors was formulated to induce and potentiate the expression of cardiac transcription factors in patient-derived hMSC while maintaining the progenitor profile of cellular proliferation at an intermediate stage that preceded induction of sarcomerogenesis. Although components of embryonic cardiogenesis were rep-

resented, the cardiogenic cocktail regimen applied here in the hMSC model system was distinct from the complex kinetics and morphogen gradients of developmental biology. Yet, this cocktail was sufficient to secure across the studied patient cohort the reparative cardiopoietic phenotype. Furthermore, there is limited evidence for the capacity of adult hMSC to execute cardiac fate despite an aptitude for in vivo transdifferentiation (12,13,15,36,41). Here, the cocktail-guided cardiopoietic phenotype demonstrated an acquired capacity for extended differentiation yielding adult stem cell–derived sarcomerogenesis and electromechanical coupling.

The present proof-of-concept study thus establishes a platform to enhance the benefit of patient-derived stem cells in treating chronic ischemic cardiomyopathy. Identifying the molecular properties of reparative hMSC in an ischemic heart disease patient cohort established criteria consistent with an aptitude for cardiac repair. Application of a recombinant inductive milieu proved sufficient to guide hMSC isolated from a coronary artery disease cohort into cardiopoiesis and, thereby, optimize efficacy prior to transplantation. Cardiogenic cocktail-induced pre-emptive cell fate specification ensured safe and lasting functional and structural benefit following transplantation in the failing ischemic heart. Within the healing murine heart, human-specific nuclear, sarcomeric, and gap junction proteins documented an active contribution to infarct repair. Moreover, up-regulation of endogenous stem cells and promotion of cell cycle activity within the host myocardium indicated a concomitant paracrine role in repair (5,34,42,43). Scaled-up GMP production of cardiopoietic hMSC indicated translational feasibility. Ultimately, the value of this technology to the patient will require controlled clinical trials.

Acknowledgment

The authors thank Dr. Allan B. Dietz, Mayo Clinic, for his contribution of platelet lysate.

Reprint requests and correspondence: Dr. Andre Terzic, Mayo Clinic, Stabile 5, 200 First Street SW, Rochester, Minnesota 55905. E-mail: terzic.andre@mayo.edu.

REFERENCES

1. Dimmeler S, Zeiher AM, Schneider MD. Unchain my heart: the scientific foundations of cardiac repair. J Clin Invest 2005;115:572–83.
2. Srivastava D, Ivey KN. Potential of stem-cell-based therapies for heart disease. Nature 2006;441:1097–9.
3. Segers VF, Lee RT. Stem-cell therapy for cardiac disease. Nature 2008;451:937–42.
4. Abdel-Latif A, Bolli R, Tleyjeh IM, et al. Adult bone marrow-derived cells for cardiac repair: a systematic review and meta-analysis. Arch Intern Med 2007;167:989–97.
5. Passier R, van Laake LW, Mummery CL. Stem-cell-based therapy and lessons from the heart. Nature 2008;453:322–9.
6. Hahn JY, Cho HJ, Kang HJ, et al. Pre-treatment of mesenchymal stem cells with a combination of growth factors enhances gap junction formation, cytoprotective effect on cardiomyocytes, and therapeutic efficacy for myocardial infarction. J Am Coll Cardiol 2008;51:933–43.
7. Hare JM, Traverse JH, Henry TD, et al. A randomized, double-blind, placebo-controlled, dose-escalation study of intravenous adult human mesenchymal stem cells (prochymal) after acute myocardial infarction. J Am Coll Cardiol 2009;54:2277–86.
8. Quevedo HC, Hatzistergos KE, Oskouei BN, et al. Allogeneic mesenchymal stem cells restore cardiac function in chronic ischemic cardiomyopathy via trilineage differentiating capacity. Proc Natl Acad Sci U S A 2009;106:14022–7.
9. Rosenzweig A. Cardiac cell therapy—mixed results from mixed cells. N Engl J Med 2006;355:1274–7.
10. Chavakis E, Urbich C, Dimmeler S. Homing and engraftment of progenitor cells: a prerequisite for cell therapy. J Mol Cell Cardiol 2008;45:514–22.
11. Dimmeler S, Leri A. Aging and disease as modifiers of efficacy of cell therapy. Circ Res 2008;102:1319–30.
12. Johnston PV, Sasano T, Mills K, et al. Engraftment, differentiation, and functional benefits of autologous cardiosphere-derived cells in porcine ischemic cardiomyopathy. Circulation 2009;120:1075–83.
13. Smith RR, Barile L, Cho HC, et al. Regenerative potential of cardiosphere-derived cells expanded from percutaneous endomyocardial biopsy specimens. Circulation 2007;115:896–908.
14. Dietz AB, Padley DJ, Gastineau DA. Infrastructure development for human cell therapy translation. Clin Pharmacol Ther 2007;82:320–4.
15. Behfar A, Perez-Terzic C, Faustino RS, et al. Cardiopoietic programming of embryonic stem cells for tumor-free heart repair. J Exp Med 2007;204:405–20.
16. Behfar A, Zingman LV, Hodgson DM, et al. Stem cell differentiation requires a paracrine pathway in the heart. FASEB J 2002;16:1558–66.
17. Plenz G, Eschert H, Erren M, et al. The interleukin-6/interleukin-6-receptor system is activated in donor hearts. J Am Coll Cardiol 2002;39:1508–12.
18. Messina E, De Angelis L, Frati G, et al. Isolation and expansion of adult cardiac stem cells from human and murine heart. Circ Res 2004;95:911–21.
19. Wobus AM, Kaomei G, Shan J, et al. Retinoic acid accelerates embryonic stem cell-derived cardiac differentiation and enhances development of ventricular cardiomyocytes. J Mol Cell Cardiol 1997;29:1525–39.
20. Perez-Terzic C, Behfar A, Mery A, van Deursen JM, Terzic A, Puceat M. Structural adaptation of the nuclear pore complex in stem cell-derived cardiomyocytes. Circ Res 2003;92:444–52.
21. Yamada S, Nelson TJ, Behfar A, Crespo-Diaz RJ, Fraidenraich D, Terzic A. Stem cell transplant into preimplantation embryo yields myocardial infarction-resistant adult phenotype. Stem Cells 2009;27:1697–705.
22. Zhou B, Ma Q, Rajagopal S, et al. Epicardial progenitors contribute to the cardiomyocyte lineage in the developing heart. Nature 2008;454:109–13.
23. Bruneau BG, Nemer G, Schmitt JP, et al. A murine model of Holt-Oram syndrome defines roles of the T-box transcription factor Tbx5 in cardiogenesis and disease. Cell 2001;106:709–21.
24. David R, Brenner C, Stieber J, et al. MesP1 drives vertebrate cardiovascular differentiation through Dkk-1-mediated blockade of Wnt-signalling. Nat Cell Biol 2008;10:338–45.
25. Olson EN, Schneider MD. Sizing up the heart: development redux in disease. Genes Dev 2003;17:1937–56.
26. Arrell DK, Niederlander NJ, Faustino RS, Behfar A, Terzic A. Cardioinductive network guiding stem cell differentiation revealed by proteomic cartography of tumor necrosis factor alpha-primed endodermal secretome. Stem Cells 2008;26:387–400.
27. Mummery C, Ward-van Oostwaard D, Doevendans P, et al. Differentiation of human embryonic stem cells to cardiomyocytes: role of coculture with visceral endoderm-like cells. Circulation 2003;107:2733–40.
28. Grepin C, Nemer G, Nemer M. Enhanced cardiogenesis in embryonic stem cells overexpressing the GATA-4 transcription factor. Development 1997;124:2387–95.
29. Beltrami AP, Barlucchi L, Torella D, et al. Adult cardiac stem cells are multipotent and support myocardial regeneration. Cell 2003;114:763–76.
30. Clavel C, Verfaillie CM. Bone-marrow-derived cells and heart repair. Curr Opin Organ Transplant 2008;13:36–43.
31. Uccelli A, Moretta L, Pistoia V. Mesenchymal stem cells in health and disease. Nat Rev Immunol 2008;8:726–36.
32. Amado LC, Schuleri KH, Saliaris AP, et al. Multimodality noninvasive imaging demonstrates in vivo cardiac regeneration after mesenchymal stem cell therapy. J Am Coll Cardiol 2006;48:2116–24.

33. Sotiropoulou PA, Perez SA, Salagianni M, Baxevanis CN, Papamichail M. Characterization of the optimal culture conditions for clinical scale production of human mesenchymal stem cells. Stem Cells 2006;24:462–71.
34. Psaltis PJ, Zannettino AC, Worthley SG, Gronthos S. Concise review: mesenchymal stromal cells: potential for cardiovascular repair. Stem Cells 2008;26:2201–10.
35. Wu SM, Chien KR, Mummery C. Origins and fates of cardiovascular progenitor cells. Cell 2008;132:537–43.
36. Behfar A, Faustino RS, Arrell DK, Dzeja PP, Perez-Terzic C, Terzic A. Guided stem cell cardiopoiesis: discovery and translation. J Mol Cell Cardiol 2008;45:523–9.
37. Faustino RS, Behfar A, Perez-Terzic C, Terzic A. Genomic chart guiding embryonic stem cell cardiopoiesis. Genome Biol 2008;9:R6.1–16.
38. Jiang Y, Jahagirdar BN, Reinhardt RL, et al. Pluripotency of mesenchymal stem cells derived from adult marrow. Nature 2002;418:41–9.
39. Liechty KW, MacKenzie TC, Shaaban AF, et al. Human mesenchymal stem cells engraft and demonstrate site-specific differentiation after in utero transplantation in sheep. Nat Med 2000;6:1282–6.
40. Orlic D, Kajstura J, Chimenti S, et al. Bone marrow cells regenerate infarcted myocardium. Nature 2001;410:701–5.
41. Bird SD, Doevendans PA, van Rooijen MA, et al. The human adult cardiomyocyte phenotype. Cardiovasc Res 2003;58:423–34.
42. Gonzalez A, Rota M, Nurzynska D, et al. Activation of cardiac progenitor cells reverses the failing heart senescent phenotype and prolongs lifespan. Circ Res 2008;102:597–606.
43. Deuse T, Peter C, Fedak PW, et al. Hepatocyte growth factor or vascular endothelial growth factor gene transfer maximizes mesenchymal stem cell-based myocardial salvage after acute myocardial infarction. Circulation 2009;120:S247–54.

Key Words: cell therapy ■ ischemic cardiomyopathy ■ heart failure ■ patient-derived ■ transplantation.

APPENDIX

For supplemental tables, figures, and videos, please see the online version of this article.